Journal of Marine Research, 46, 399–428, 1988

Phytoplankton species composition and abundance in a Gulf Stream warm core ring. II. Distributional patterns

by Richard W. Gould, Jr.[1,2] and Greta A. Fryxell[1]

ABSTRACT

During the spring and summer of 1982, Gulf Stream warm core ring (WCR) 82B was sampled during four cruises from April to August to investigate phytoplankton distributional patterns. Discrete water samples from 28 stations were collected for identification and enumeration of phytoplankton.

In April, when the water column was well mixed to 350 m, quantitative samples clustered by station when the 100 most frequently observed taxa were used as variables, indicating fairly unique assemblages at each station that were consistent with depth. Two transects across the ring in June showed a symmetrical diatom abundance maximum, dominated by *Chaetoceros* cf. *vixvisibilis* (maximum abundance 31,900 cells l^{-1}) and *Leptocylindrus danicus* (maximum abundance 21,000 cells l^{-1}), situated in the surface water at ring center. Dinoflagellate and coccolithophorid maxima were situated slightly deeper than the diatom maximum, in the seasonal thermocline from 20 to 35 m. A biomass maximum observed in a Shelf Water entrainment feature wrapping around the eastern perimeter of the ring contained elevated numbers of coccolithophorids and coccoid, unicellular monads (1–3 μm in diameter) and was thus compositionally distinct from the ring center biomass maximum. In July and August the ring underwent numerous interactions with and overwashes by the Slope Water and Gulf Stream. August samples from the ring, Sargasso Sea, Gulf Stream, and Slope Water all contained similar taxa and abundances.

Different phytoplankton groups may be responding to different nutrient input mechanisms at the ring edge and center. Diatom maxima at ring center may form as a result of pulsed nutrient input from storms and a slight upwelling due to the gradual relaxation of the thermocline as the ring ages, while concentrations of ultraplanktonic algae (monads, coccolithophorids) toward the ring margin may result from near steady-state nutrient input along sloping isopycnals and/or advection from the ring exterior.

1. Introduction

The biological, chemical, and physical processes occurring in Gulf Stream rings (both cold core and warm core) have been studied intensively in the past decade. There have been dramatic strides in our understanding since the 1930's and 1940's, when hydrographic data from the Gulf Stream region clearly showed the presence of rings

1. Department of Oceanography, Texas A&M University, College Station, Texas, 77843, U.S.A.
2. Present address: Oceanography Division, Code 333, Naval Ocean Research and Development Activity, NSTL, Mississippi, 39529, U.S.A.

(Iselin, 1936; Fuglister and Worthington, 1947; Iselin and Fuglister, 1948). Additional surveys of the physical structure of rings in the 1950's and 1960's (Fuglister and Worthington, 1951; Fuglister, 1963; Barrett, 1971; Parker, 1971; Fuglister, 1972, 1977) led to the large, interdisciplinary studies of cold core rings in the mid 1970's (The Ring Group, 1981) and warm core rings in the early 1980's (The Warm Core Rings Executive Committee, 1982).

Rings are not restricted to the Gulf Stream region. They are ubiquitous features and have been observed in many other areas of the world ocean: in the East Australian current system off Australia (Nilsson and Cresswell, 1981), near the Kuroshio/Oyashio fronts off Japan (Tomosada, 1975), off New Zealand (Bradford *et al.*, 1982), California (Simpson *et al.*, 1984), Florida (Yoder *et al.*, 1981), South Africa (Lutjeharms, 1981), Somalia (Bruce, 1979), in the Gulf of Mexico (Kirwan *et al.*, 1984), and in the arctic and antarctic regions (Newton *et al.*, 1974; Joyce and Patterson, 1977). The rings off the coasts of Japan and Australia have been particularly well studied and allow for regional comparisons.

There are many similarities between the rings from the Gulf Stream, Kuroshio, and East Australian Currents. For example: (1) the rings can have greater phytoplankton biomass inside than outside, depending on the season (Tranter *et al.*, 1980; Joyce *et al.*, 1984; Hitchcock *et al.*, 1985); (2) within the ring, phytoplankton (particularly diatoms) is often concentrated at the center (Jeffrey and Hallegraeff, 1980; Scott, 1981; Nelson *et al.*, 1985; Fryxell *et al.*, 1985), but enhanced biomass has also been observed at ring fronts (Hoge and Swift, 1983; Tranter *et al.*, 1983); (3) formation processes are similar—meanders pinch off from a main current (Tomosada, 1978; Nilsson and Cresswell, 1981; Joyce and Wiebe, 1983); (4) rings from all three systems are frequently reabsorbed by the currents that shed them, but the Kuroshio and Australian rings also decay through mixing with the surroundings (Nilsson and Cresswell, 1981; Joyce and Wiebe, 1983; Tomosada, 1986); (5) the warm rings may be steered or trapped by bottom topography in all three regions (Nilsson and Cresswell, 1981; Evans *et al.*, 1985; Tomosada, 1986); (6) entrainment features and overwashes are not uncommon (Tomosada, 1978; Tranter *et al.*, 1982; Joyce *et al.*, 1983, 1984); and (7) deep convective mixing in the ring in the winter can be followed by summer capping (Tomosada, 1978; Nilsson and Cresswell, 1981; Tranter *et al.*, 1982; Mulhearn, 1983; Nelson *et al.*, 1985).

Differences exist as well, however: (1) the Australian rings are most intense near shore and drift southward in complex loops, while the Gulf Stream rings form along much of the northern edge of the Gulf Stream and drift back toward shore, and the Kuroshio rings drift poleward (Nilsson and Cresswell, 1981; Joyce and Wiebe, 1983; Tomosada, 1986); (2) cold core rings are frequently observed in the Gulf Stream and Kuroshio regions, rarely off Australia (Forbes, 1982); (3) reseparation from the current system has been observed for approximately 40% of the warm core rings in the Kuroshio region, but has only occasionally been observed in the Australian system and

has never been observed in the Gulf Stream region (Tomosada, 1986); (4) multi-core structures have been found in Kuroshio and Australian warm core rings, but not in the ones from the Gulf Stream (Tomosada, 1986; Cresswell and Legeckis, 1986).

From April to August, 1982, WCR 82B was tracked by satellite (Evans *et al.*, 1985) and sampled periodically on three multiple-ship cruises (and one ship-of-opportunity cruise) throughout the five month period. The ring was approximately two months old at the onset of the study. Our objective here is to examine the horizontal and vertical distribution of phytoplankton in and around WCR 82B. This study provided an opportunity to examine the distributions of phytoplankton groups and individual species in three distinct water masses in the northwest Atlantic Ocean.

2. Methods

Although phytoplankton biomass is typically expressed as chlorophyll concentration, biomass estimates can also be obtained more directly, through microscopic observation and enumeration, as in this study. Although this method is very labor intensive, it not only provides information concerning the amount of carbon available for transfer into higher trophic levels, but also provides autecological and synecological information regarding phytoplankton species. The data are in terms of reproducing units, which is also helpful.

See Gould and Fryxell (part I, 1988, this issue) for a description of sample locations (their Fig. 1 and Table 1) and collection and analytical procedures. All samples discussed here are whole water samples collected with Niskin bottles on a CTD rosette sampling system (see Gould, 1988, for a discussion of net phytoplankton samples).

Twenty eight stations were occupied during the five month study, including fourteen stations along two transects in June. The transects formed a slightly distored "X" pattern and provided horizontal coverage across the ring. Six stations were occupied along a northwest to southeast transect on 16 and 17 June, and eight stations on a northeast to southwest transect a week later on 23–25 June. Station 20 along the second transect was located in a Shelf Water entrainment feature that wrapped around the eastern perimeter of the ring (Fig. 1). The first transect passed about 50 km north of the ring center, but the second passed almost directly through it (Fig. 1).

The taxa observed were assigned to one of four major phytoplankton groups: diatoms, dinoflagellates, coccolithophorids, or other algae. The "other" category contains all cells not contained in the first three categories. Included are silicoflagellates, chlorophytes, prymnesiophytes, cryptophytes, chrysophytes, prasinophytes, and cyanophytes. As mentiond in Gould and Fryxell (part I, 1988, this issue), the dominant component in the "other" group in all samples was a coccoid, unicellular monad (without flagella in the preserved samples) approximately 1–3 μm in diameter (could be considered in *Synechococcus* or *Chlorella* complexes).

The quantitative phytoplankton estimates are compared here to assess intracruise

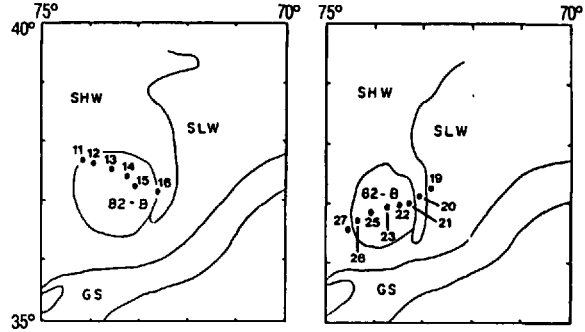

Figure 1. Station locations along the two ring transects in June. A. First transect, 16–17 June, 1982. B. Second transect, 23–25 June, 1982. GS is Gulf Stream, SHW is Shelf Water, and SLW is Slope Water. Station numbers correspond to locations in Table 1 and Figure 1 in Gould and Fryxell, part I (this issue).

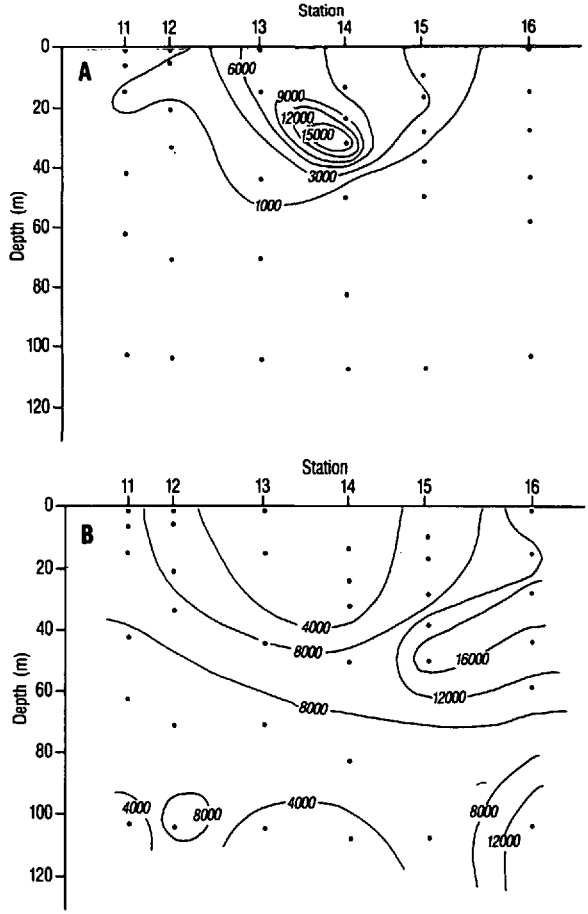

Figure 2. Vertical distribution of diatoms and coccolithophorids, first transect, 16–17 June. A. Diatoms. B. Coccolithophorids. Abundances in cells l^{-1}.

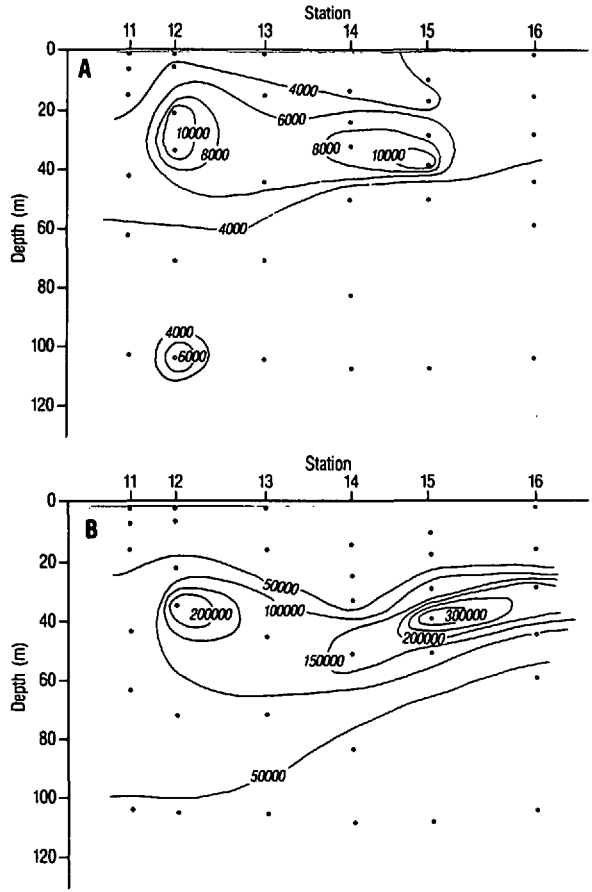

Figure 3. Vertical distribution of dinoflagellates and other algae, first transect, 16–17 June. A. Dinoflagellates. B. Other algae. Abundances in cells l^{-1}.

spatial variability in phytoplankton abundance in and around WCR 82B. All principal component analyses (PCA) were done with the Statistical Analysis System (SAS) and are based on the correlation matrix.

The CTD data (temperature, salinity, oxygen) were collected by T. Joyce.

3. Results

In June, horizontal phytoplankton distributions across the ring were obtained from two transects. Figures 2–5 are contour plots of diatoms, coccolithophorids, dinoflagellates, other algae, temperature, salinity, density, and oxygen for the first transect, 16-17 June. Figures 6–9 are contour plots of the same variables for the second transect, 23-25 June. Recall that the first transect passed about 50 km north of the ring center. In both transects diatoms were concentrated in the surface waters toward the center of

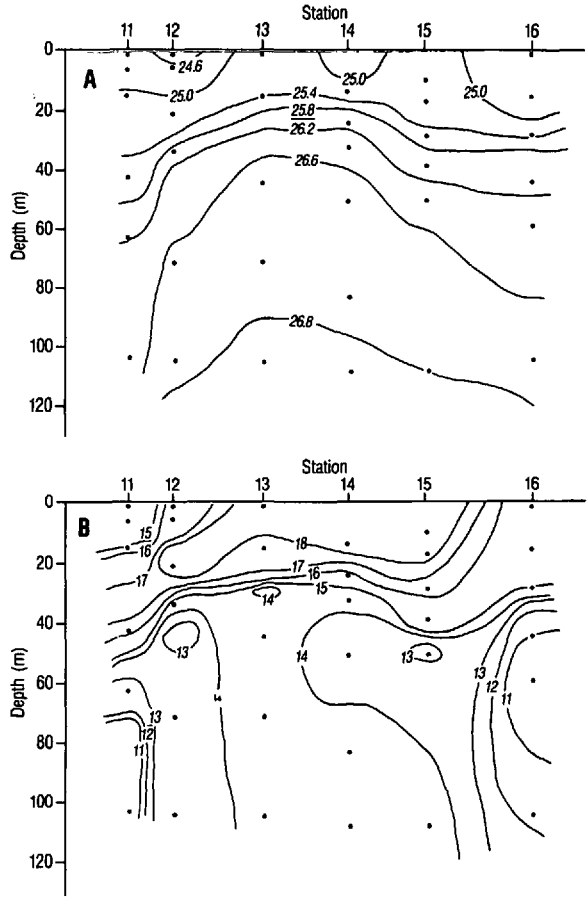

Figure 4. Vertical distribution of density and temperature, first transect, 16–17 June. A. Density (σ_θ). B. Temperature (°C.).

the ring, and were observed in very low abundances below about 40 m (Figs. 2A, 6A). The consistency of the diatom maximum at ring center over the ten day period during which the transects were run suggests that it was a fairly stable feature temporally and spatially.

Coccolithophorids were generally observed in highest numbers toward the edges of the ring (Figs. 2B, 6B); however, high cell densities were also observed at ring center of the second transect, below the diatom maximum (Fig. 6B). Dinoflagellates had subsurface maxima in the 20–40 m depth range, just inside the ring edges along transect one (Fig. 3A) and toward the center of transect two (Fig. 7A).

The other algae also exhibited subsurface maxima, at the same stations and depths as the dinoflagellates along transect one (Fig. 3B), and at the southwest edge of the ring and in the entrainment feature (station 20) along transect two (Fig. 7B).

In the ring interior a sharp pycnocline was located in the 20–35 m depth range (Figs.

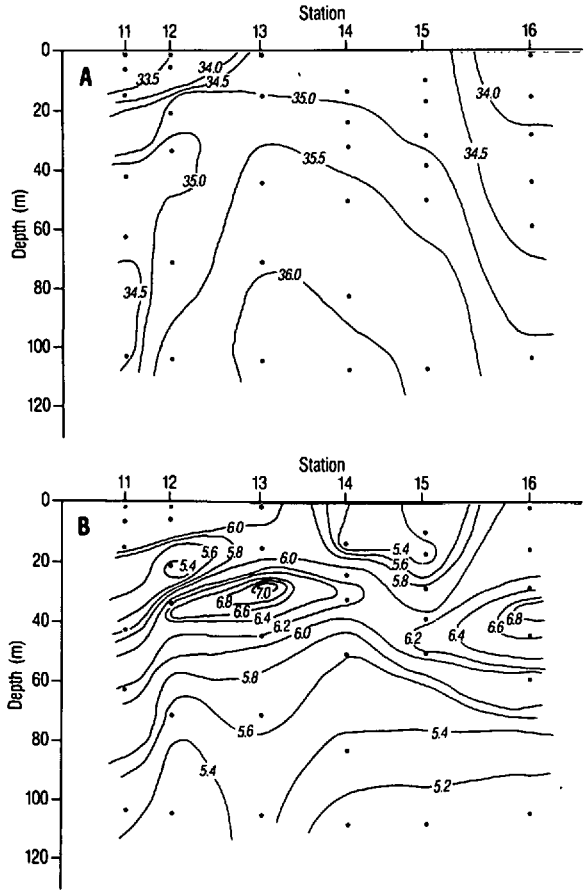

Figure 5. Vertical distribution of salinity and oxygen, first transect, 16–17 June. A. Salinity (‰). B. Oxygen (ml l^{-1}).

4A, 8A). Colder temperatures and lower salinities were found toward the edges of the ring and in the shelf water entrainment feature on transect two (Figs. 4B, 5A, 8B, 9A). Oxygen maxima were generally located in the pycnocline, except for station 23 at the center of transect two, where a surface maximum was observed (Figs. 5B, 9B). The oxygen maximum at the southeast edge of transect one (stations 15 and 16) corresponded with high numbers of coccolithophorids and other algae. The oxygen maximum at stations 12, 13, and 14 coincided with high numbers of diatoms, dinoflagellates, and other algae. Along transect two, the pycnocline oxygen maxima toward both edges of the ring appeared to be related to high densities of coccolithophorids and other algae, while the surface ring center maximum fell in an area of high diatom, dinoflagellate, and coccolithophorid numbers.

The small, unicellular, coccoid monad that dominated most of the samples was abundant in the upper 20 m of the ring in April (33,000–117,000 cells l^{-1}). Lower

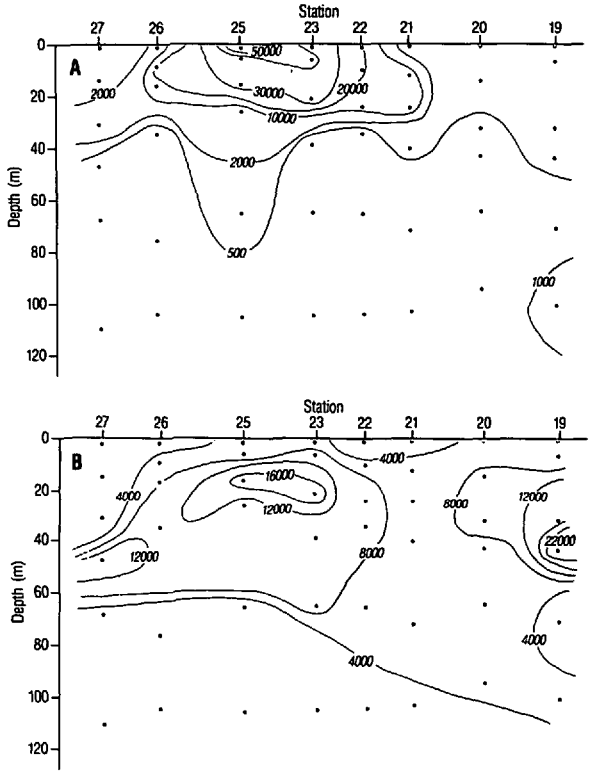

Figure 6. Vertical distribution of diatoms and coccolithophorids, second transect, 23–25 June. A. Diatoms. B. Coccolithophorids. Abundances in cells l^{-1}.

numbers (7,700–28,000 cells l^{-1}) were observed at the Sargasso Sea station. By June, maximum monad abundances had shifted deeper in the water column, below the thermocline, in the 30–70 m depth range (Fig. 10). The Slope station also had high numbers, but again, relatively few monads were observed in the Sargasso Sea samples. Lower numbers were generally observed in August, but the maximum remained deep in the water column. The Sargasso Sea and Gulf Stream still had lower numbers (3,000–19,000 cells l^{-1}) than the Slope Water station or the first ring center station (10,000–190,000 cells l^{-1}).

The diatoms *Chaetoceros* cf. *vixvisibilis* and *Leptocylindrus danicus* showed similar patterns of distribution. Both species were observed at scattered locations in low abundances in April, but in June they were both concentrated in the surface water at ring center, with *C.* cf. *vixvisibilis* present at abundances as high as 31,900 cells l^{-1} and *L. danicus* at 21,600 cells l^{-1}. Figure 11 shows their distributions along the second transect in June. Few cells, if any, were observed in the unconcentrated samples from the edge and entrainment stations or from the deeper samples (> 30 m).

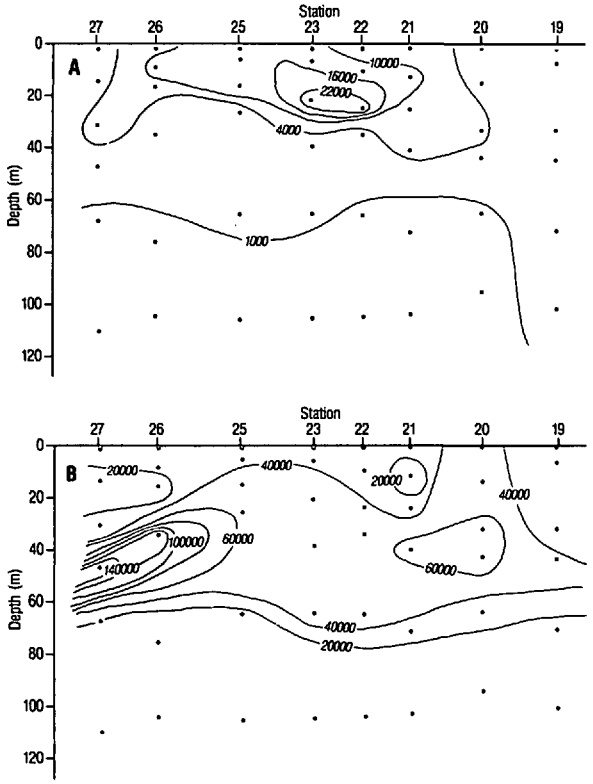

Figure 7. Vertical distribution of dinoflagellates and other algae, second transect, 23–25 June. A. Dinoflagellates. B. Other algae. Abundances in cells l^{-1}.

Two other taxa that had similar distribution patterns were the coccolithophorid *Calyptrosphaera catillifera* and a small, lightly thecate dinoflagellate (*Gonyaulax* sp. "A"). In April, neither taxon was very abundant or frequently observed in the ring (*C. catillifera* was only observed in seven samples from the April/May cruise at a maximum abundance of 620 cells l^{-1}; *Gonyaulax* sp. "A" was seen in ten samples at a maximum abundance of 930 cells l^{-1}), but both were somewhat more common in the Sargasso Sea. In June, both taxa were concentrated in the upper 30 m toward the center of the second transect (Fig. 12); however, the small dinoflagellate was fairly abundant at the Slope (maximum abundance was 5,900 cells l^{-1}) and Sargasso Sea (maximum was 3,000 cells l^{-1}) stations as well. The maximum abundance of both taxa in August was at 41 m at the ring center station on the 9th (*C. catillifera*, 2,900 cells l^{-1}; *G.* sp. "A", 19,200 cells l^{-1}). *Calyptrosphaera catillifera* was also seen at the Sargasso Sea station at concentrations of several hundred cells l^{-1}. *Gonyaulax* sp. "A" was observed in nearly every sample in August at concentrations from several hundred to several thousand cells l^{-1}.

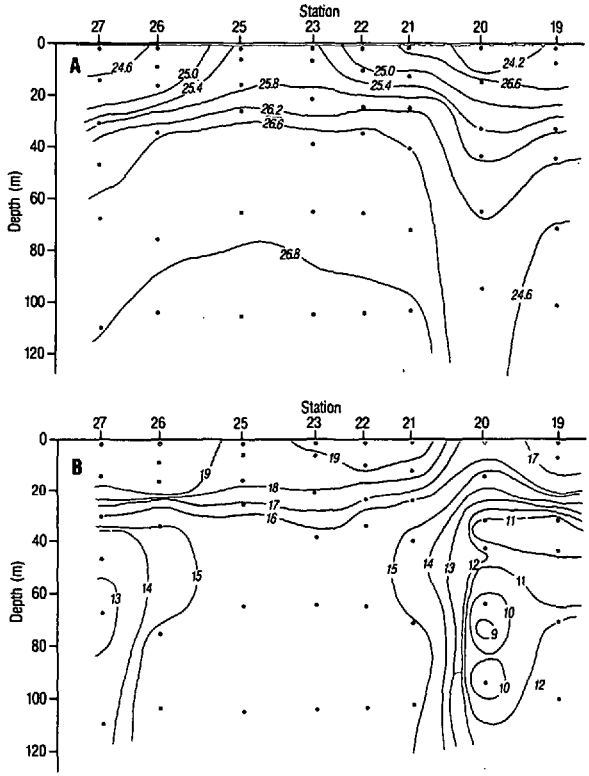

Figure 8. Vertical distribution of density and temperature, second transect, 23–25 June. A. Density (σ_θ). B. Temperature (°C.).

Emiliania huxleyi was the most abundant and most frequently observed coccolithophorid during the sampling period. In April and May, it was observed in greatest abundance at the ring edge and Sargasso Sea stations, relative to the ring center (Fig. 13). In June, it was more abundant at the Slope, ring edge, and entrainment stations than at the ring center or Sargasso Sea stations (Fig. 14). Within the ring, however, it was relatively more abundant in the thermocline along the second transect. In August, all the samples had similar abundances of *E. huxleyi,* except for a peak at the third depth at the first ring center station (809.07).

To investigate intracruise spatial patterns, PCA was performed separately on the data from each cruise using the most frequently observed taxa (present in at least 10% of the samples for a given cruise) as variables. A total of 100 taxa met this criterion (Appendix).

In April, the first three principal components accounted for 28.9% of the variability in the data. Examination of the eigenvectors provides information as to which species played a role in determining station and sample differences. High loadings were given to the following taxa on component one: *Syracosphaera pulchra, Nitzschia closter-*

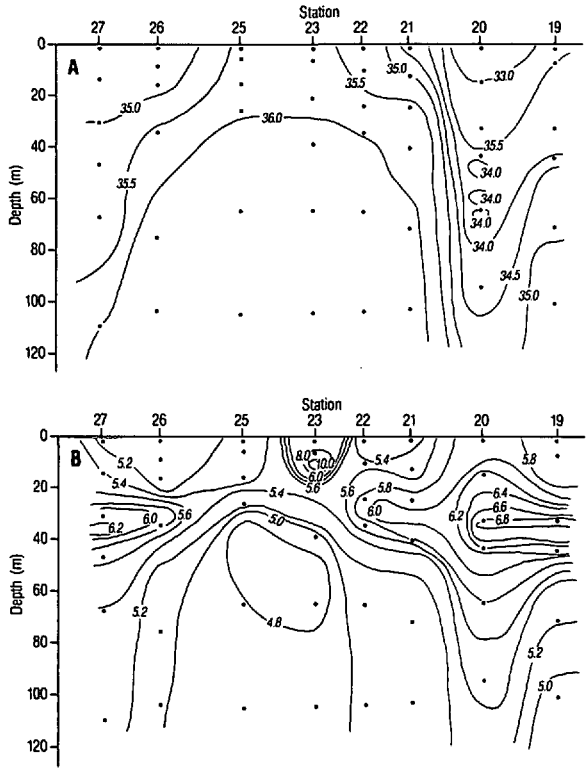

Figure 9. Vertical distribution of salinity and oxygen, second transect, 23–25 June. A. Salinity (‰). B. Oxygen (ml l^{-1}).

ium, Calciosolenia murrayi, Periphyllophora mirabilis, Phaeocystis spp., *Gonyaulax* sp. "A", *Calyptrolithophora gracillima, Laminolithus marsilii, Chaetoceros breve, Anoplosolenia brasiliensis, Bacteriastrum* spp., and *Chaetoceros* spp. On the second component, high loadings were given to: *Emiliania huxleyi, Minidiscus trioculatus, Thalassiosira bulbosa* ?, *Protoperidinium bipes,* undetermined centric, undetermined pennate, yellow cell, and undetermined flagellates.

Scores of the first two principal components from the April analysis are plotted in Figure 15. At stations 426.01, 426.06, 501.02, and 504.01 the nine depths sampled corresponded to the light levels reported in the Methods section of Gould and Fryxell (part I, 1988, this issue). At 429.01, 12 depths were sampled, but at 519.01 only three samples were collected (12, 36, 70 m) and at 603.01 only two (2 and 10 m). The symbols plotted in Figure 15A represent stations. In this analysis, events 426.01 (A—ring center), 501.02 (D—Sargasso Sea), and 504.01 (E—ring center) were fairly distinct, while 426.06 (B—second ring center) and 429.01 (C—ring edge) clustered together. Because the species and abundances at the second ring center station were similar to those at the ring edge station, the supposition that advection from the ring

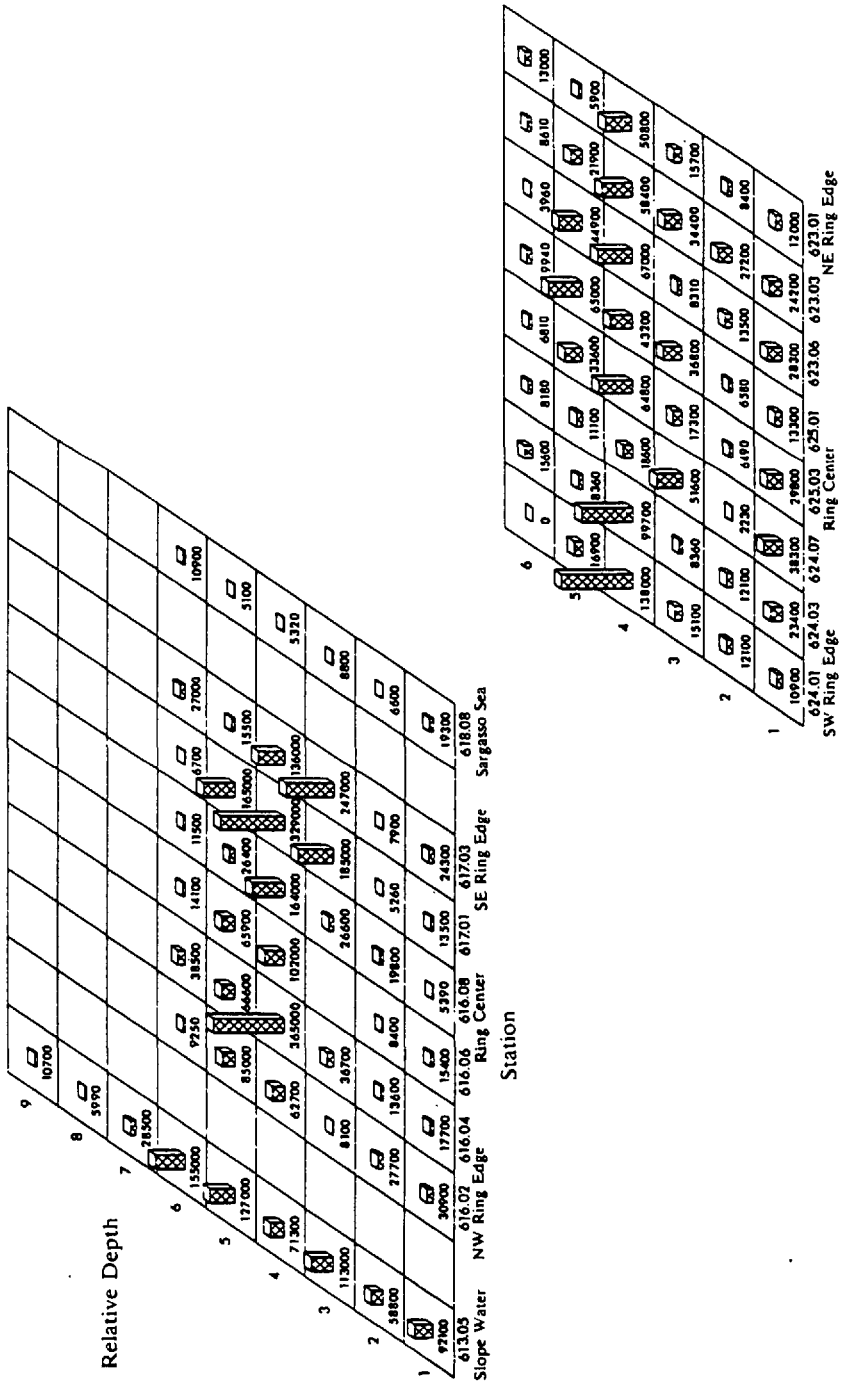

Figure 10. Vertical distribution of monads along the two transects, June. Abundances in cells l^{-1}. Note the different abundance scales.

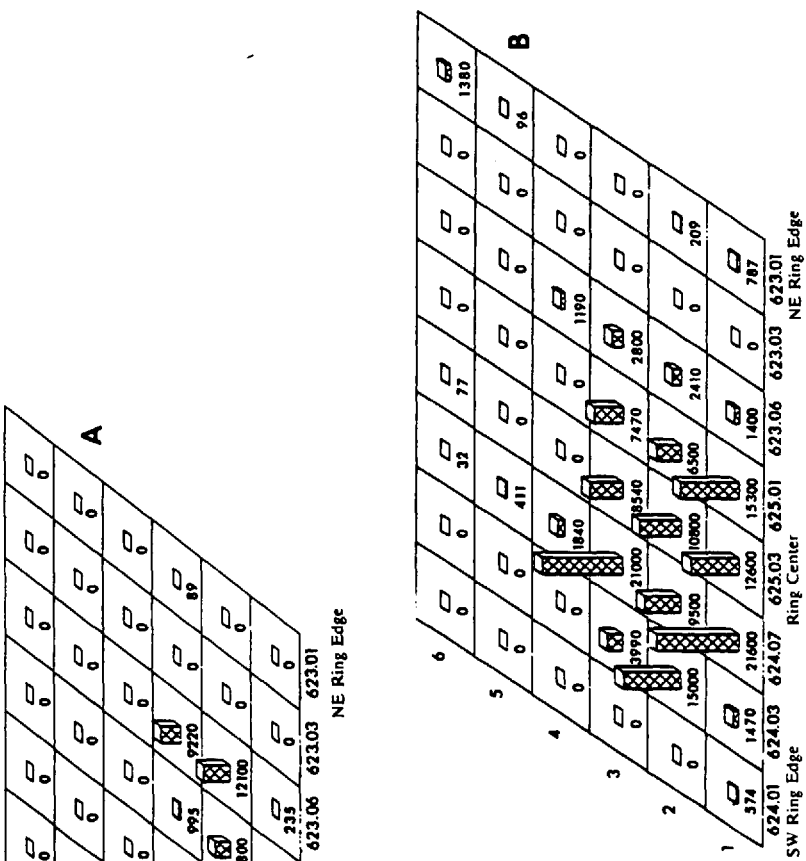

Figure 11. Vertical distribution of *Chaetoceros* cf. *vixvisibilis* and *Leptocylindrus danicus*, second transect, 23–25 June. A. *C.* cf. *vixvisibilis*. B. *L. danicus*. Abundances in cells l^{-1}. Note the different abundance scales.

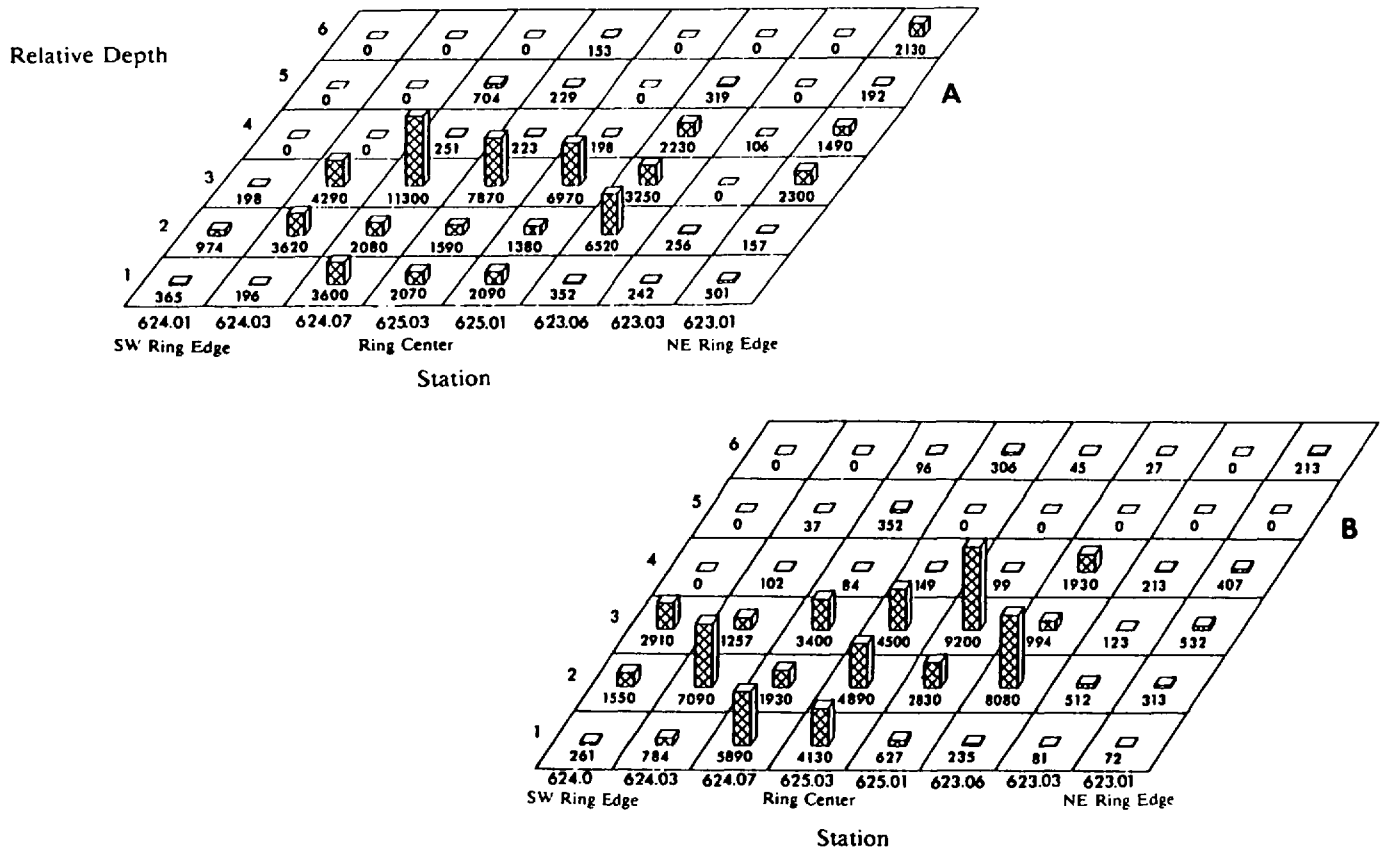

Figure 12. Vertical distribution of *Calyptrosphaera catillifera* and *Gonyaulax* sp. "A," second transect, 23–25 June. A. *C. catillifera*. B. *G.* sp. "A." Abundances in cells l^{-1}. Note the different abundance scales.

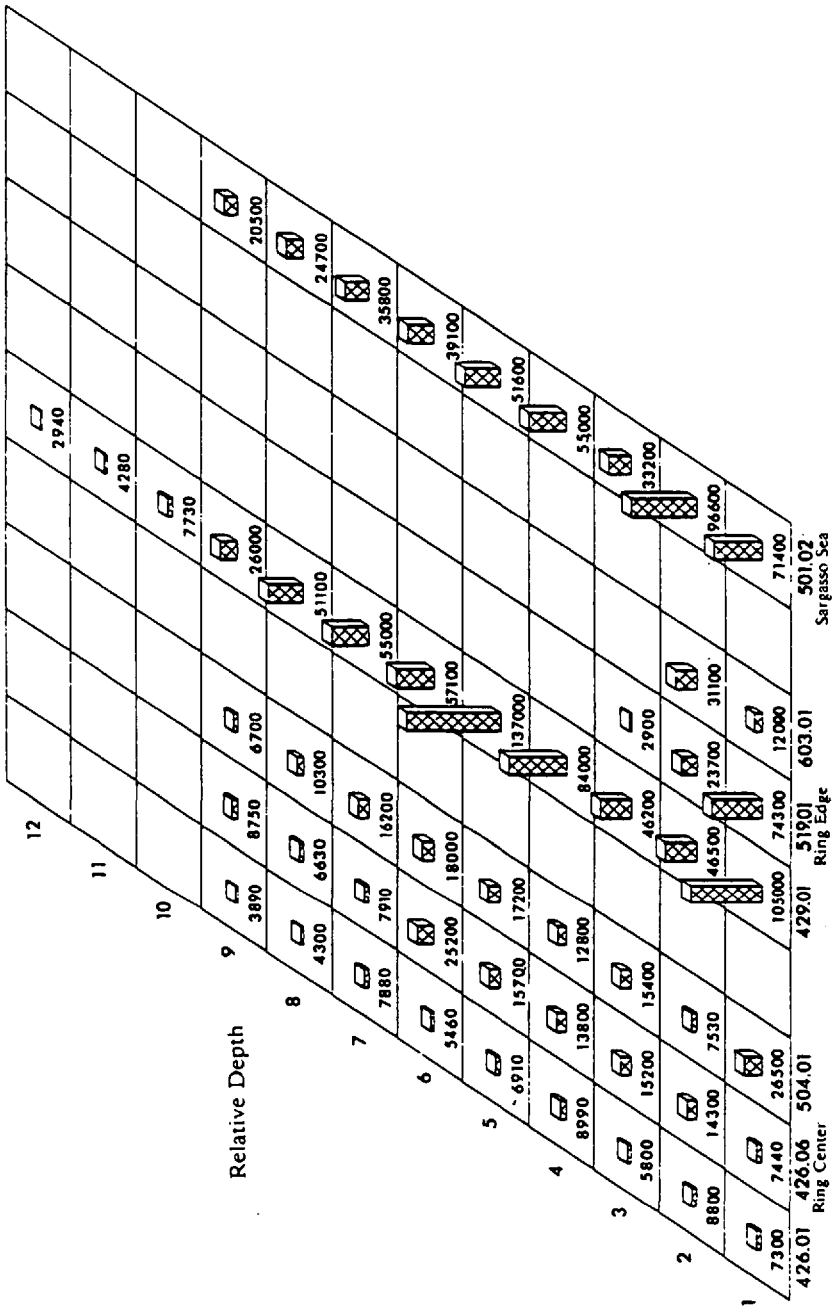

Figure 13. Vertical distribution of *Emiliania huxleyi*, April. Abundances in cells l^{-1}.

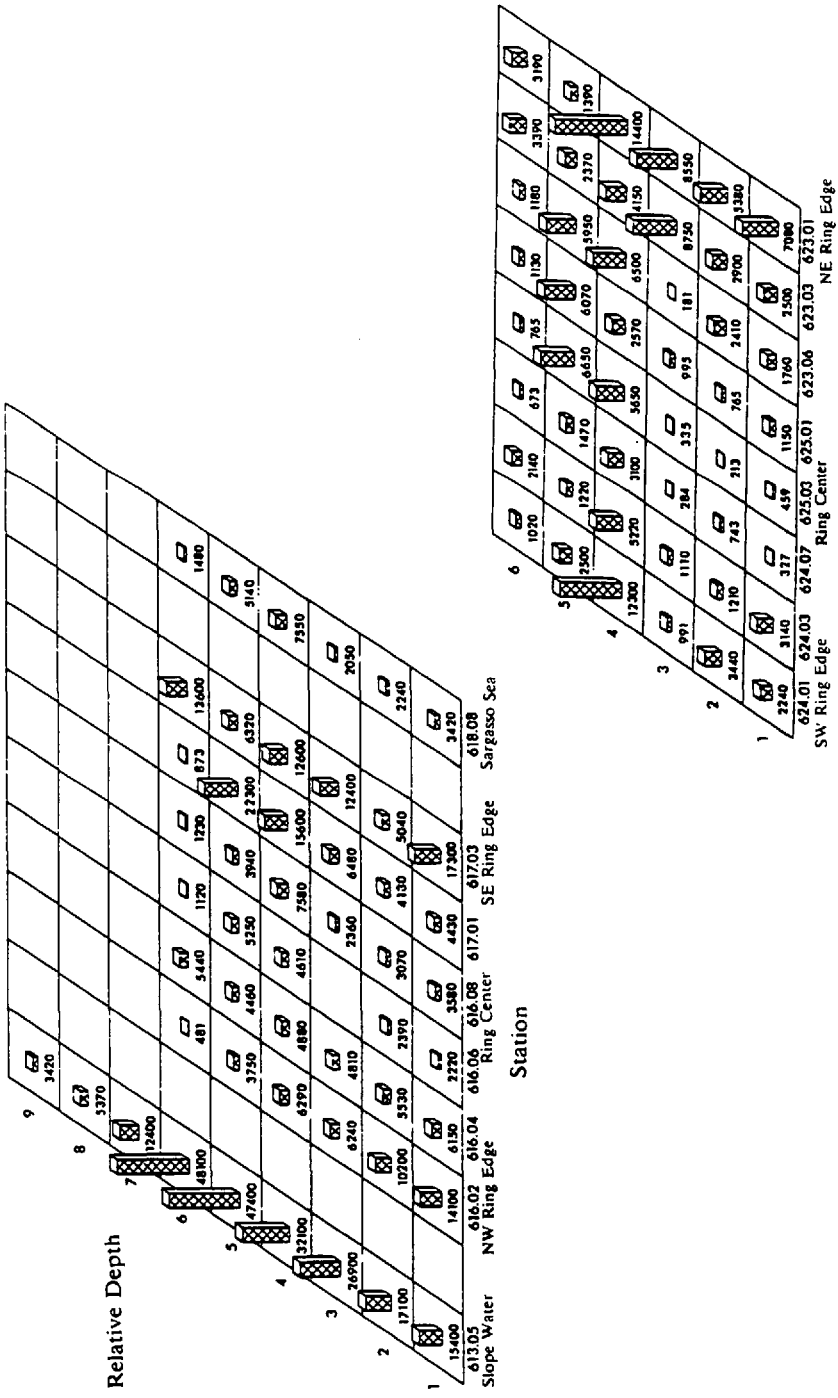

Figure 14. Vertical distribution of *Emiliania huxleyi* along the two transects, June. Abundances in cells l^{-1}. Note the different abundance scales.

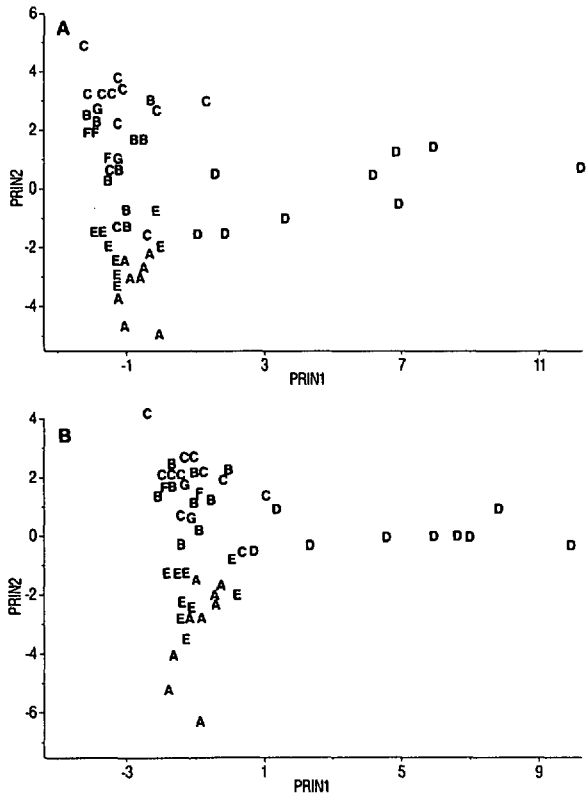

Figure 15. Principal component analysis using the 100 most frequently observed taxa as variables, natural-log abundance and presence/absence data, April. Symbols represent stations: A—426.01, ring center; B—426.06, ring center; C—429.01, ring edge; D—501.02, Sargasso Sea; E—504.01, ring center; F—519.01, ring edge; G—603.01, ring edge. A. Natural-log abundance data. B. Presence/absence data.

periphery was responsible for the differences observed between the two ring center stations on 26 April (one in the morning and one in the afternoon) is supported (see Gould and Fryxell, part I, this volume). Also, the Sargasso Sea station separated from the other stations due to high abundances of the species that were given high loadings on the first principal component axis (listed above), while the other stations separated due to differences in abundance of the species that were given high loadings on the second axis (also listed above).

When presence/absence data of the most frequently observed taxa were used instead of natural-log transformed abundances, similar groupings were observed (Fig. 15B). Events 426.01, 501.02, and 504.01 were fairly distinct, indicating that the differences between these stations and the others could be resolved at the level of presence or absence of these species. The differences in abundance simply served to reinforce the patterns.

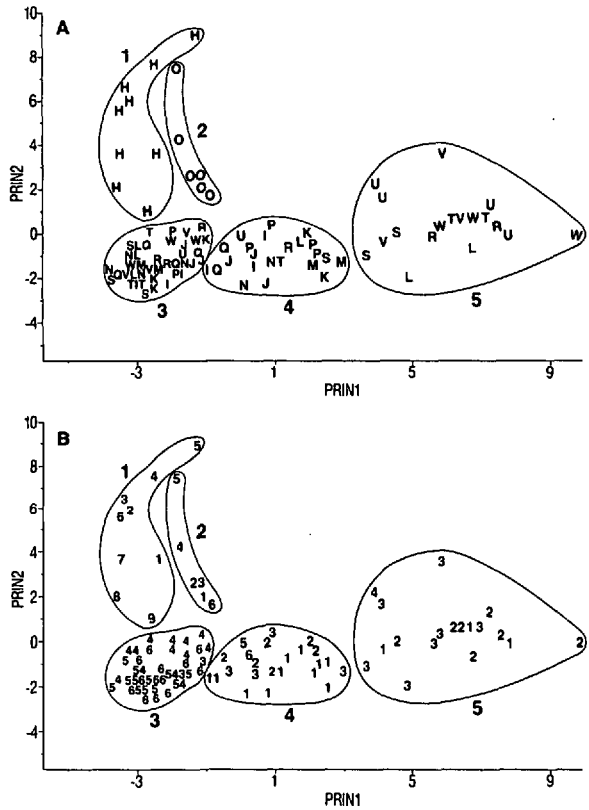

Figure 16. Principal component analysis using the 100 most frequently observed taxa as variables, natural-log abundance data, June. Circumscriptions are subjective to help show patterns (see text). A. Symbols represent stations: H—613.05, Slope Water; I—616.02, T1 (transect one); J—616.04, T1; K—616.06, T1; L—616.08, T1; M—617.01, T1; N—617.03, T1; O—618.08, Sargasso Sea; P—623.01, T2 (transect two); Q—623.03, T2; R—623.06, T2; S—624.01, T2; T—624.03, T2; U—624.07, ring center; V—625.01, T2; W—625.03, ring center. B. Symbols represent relative depth. Relative depth 1 is the shallowest sample at a station.

In the June analysis using natural-log transformed data on the most frequently observed species, the first three principal components accounted for 23.9% of the variance. The first principal component had high loadings for *Chaetoceros* cf. *vixvisibilis, Leptocylindrus danicus, Calyptrosphaera catillifera, Nitzschia closterium, Thalassiothrix mediterranea, Haslea wawrikae,* and *Triadinium sphaericum,* while the second one had high loadings for *Phaeocystis* spp., *Caneosphaera molischii, Minidiscus trioculatus, Helicosphaera hyalina, Coronosphaera mediterranea,* eucaryotic cell, *Gonyaulax* sp. "A", *Anthosphaera oryza,* and *Calciosolenia murrayi.*

The two plots in Figure 16 are identical but in Figure 16A, the symbols represent the stations from which the samples came, while in the bottom plot (Fig. 16B) they

represent relative depth. Relative depth 1 at a station is the shallowest. The circumscriptions are subjective but help to delineate patterns. For example, in group 2, we see from Figure 16A that all the samples are from the Sargasso Sea station (designated by the O's); from Figure 16B, we see that the samples are from relative depths 1–6. The nine depths sampled at station 613.05 corresponded to the light levels reported in the Methods section of Gould and Fryxell (part I, 1988, this issue); six depths were sampled at all other June stations.

Two stations clustered separately, 613.05, the Slope Water station, and 618.08, the Sargasso Sea station, with higher scores on the second principal component axis (i.e., greater abundances of the taxa that were given high loadings on the second axis). In June, samples from ring stations intermingled (groups 4, 5, and 6 in Fig. 16A), indicating similar species and abundances at those stations, and gradual, not disjunct changes. The ring samples separated more by sample depth rather than by station, as indicated in Figure 16B. Located at the right end of the first axis were the surface samples from stations near ring center (group 5). These samples contained large abundances of the species that had high loadings on the first principal component axis. Toward the middle of the first axis were surface samples away from ring center (group 4), and at the left end of the axis were the deep samples (group 3). Thus, ring samples separated based on depth, but they also separated based on location within the ring (edge vs. center). The same patterns were apparent using only presence/absence data of the most frequently observed taxa. Thus, variability across the ring and with depth resulted from differences in the species present in the samples, as well as from differences in abundance.

The first three principal components in the August analysis accounted for 30.1% of the variation in the data. Nine depths were sampled at stations 809.07, 812.03, and 813.02. At 818.04 six samples were collected from the water column and at 815.06, only three. The first two principal component axes are plotted in Figure 17.

The first axis appears to be a depth axis, with shallower samples displaced in the positive direction and deeper ones in the negative. The shallower samples had greater abundances of *Oxytoxum variabile, Glenodinium danicum, Helladosphaera cornifera, Gymnodiniaceae,* undertermined flagellates, and eucaryotic cells than the deeper samples (these were the taxa with high loadings on the first principal component). The Sargasso Sea and Gulf Stream stations (symbols Z and #, respectively, in Fig. 17A) separated slightly from the others with higher scores on the second axis, due to larger numbers of *Umbellosphaera tenuis, Oxytoxum variabile, Nitzschia sicula, Florosphaera profunda, Thorosphaera flabellata, Rhizosolenia delicatula,* prasinophytes, and *Gonyaulax* sp. "A," relative to the other samples. There were only minor differences between any of the August samples based on abundances of the most frequently observed taxa, however, as evidenced by the intermingling of samples from different stations and the lack of any distinct sample groups.

The presence of *Biddulphia alternans* (Bailey) Van Heurck, *Biddulphia mobilien-*

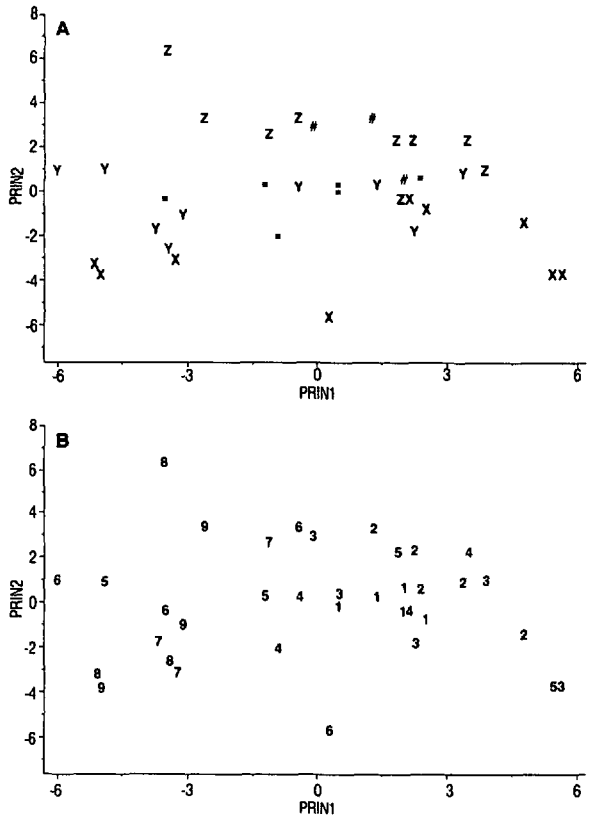

Figure 17. Principal component analysis using the 100 most frequently observed taxa as variables, natural-log abundance data, August. A. Symbols represent stations: X—809.07, ring center; Y—812.03, ring center; Z—813.02, Sargasso Sea; #—815.06, Gulf Stream; *—818.04, Slope Water. B. Symbols represent relative depth. Relative depth 1 is the shallowest sample at a station.

sis Bailey, *Cymatosira lorenzianum* Grunow, and *Paralia sulcata* (Ehrenberg) Cleve in the ring, common neritic and/or tychoplanktonic diatom species (Marshall, 1982; Marshall and Cohn, 1982, 1987a; Tester and Steidinger, 1979), indicates the penetration of Shelf and Slope Water into the ring, and satellite imagery clearly showed numerous Gulf Stream interactions with the ring in July and August (Evans *et al.*, 1985). Thus the similarity of the samples can be explained.

4. Discussion

a. Phytoplankton distributional patterns. Analyses using either species abundances or species presence/absence showed the April/May samples to cluster by station, so differences between the stations were apparent at the level of species composition and were reinforced by differences in abundance.

Two biomass maxima in June were described by Nelson *et al.* (1985) based on chlorophyll, ATP, biogenic silica, phytoplankton cell counts, and particulate organic carbon; one was at ring center and one was in the Shelf Water entrainment feature that was wrapping around the northeastern perimeter of the ring (station 20; see Fig. 1B). The maxima were compositionally distinct and the authors argued that the ring center biomass accumulation was the result of *in situ* growth and not simply particle concentration by the flow field. Phytoplankton species composition, biogenic silica concentration, and small particle concentration were used to support the hypothesis. An estimated maximal exchange rate between the Slope Water and ring core was coupled with a maximum biogenic silica concentration for the Slope Water, and it was found that a simple influx of Slope Water could not account for the high silica content of the ring core; cell growth was required. Also, if the flow field of the ring served to concentrate particles at the center, then all particles should exhibit maximum concentrations there. This was not the case. Monads in the 1–3 μm size range were more abundant in the entrainment feature and toward the ring perimeter than at ring center (this was also true for bacteria).

In the ring center biomass maximum in June, diatoms were extremely abundant in the upper 20 m (>50,000 cells l^{-1}, Fig. 6A), while dinoflagellates and coccolithophorids had abundance maxima slightly deeper, embedded in the thermocline (27,000 and 18,000 cells l^{-1}, respectively, Figs. 6B, 7A). The most abundant diatoms in the ring center biomass maximum were *Chaetoceros* cf. *vixvisibilis, Leptocylindrus danicus, Nitzschia pseudodelicatissima, Nitzschia subfraudulenta, Nitzschia closterium,* and *Thalassiothrix mediterranea;* the most abundant dinoflagellates were Gymnodiniaceae, *Gonyaulax* sp. "A", *Prorocentrum* spp., and *Triadinium sphaericum;* and the most abundant coccolithophorids were *Calyptrosphaera catillifera* and *Periphyllophora mirabilis* toward the surface and in the thermocline and *Emiliania huxleyi* slightly deeper.

In the biomass maximum at the Shelf Water entrainment station in June, diatoms were not observed in concentrations exceeding 650 cells l^{-1} in any of the samples, but small coccolithophorids and monads reached abundances up to 11,000 and 63,000 cells l^{-1}, respectively. The most abundant dinoflagellates were similar to those observed at ring center, members of the genus *Prorocentrum,* Gymnodiniaceae, and *Gonyaulax* sp. "A." *Emiliania huxleyi* was also fairly abundant there, as was the even smaller coccolithophorid *Gephyrocapsa ericsonii.* Monads were 2–5 times more abundant in the entrainment maximum than in the ring center maximum. Thus, different phytoplankton groups dominated in the two biomass maxima.

The coccoid, unicellular monads did settle in the Utermohl chambers and we feel confident with the patterns of relative abundance; the absolute abundances of these small cells might have been underestimated, however, if some cells remained unsettled or were destroyed by the preservative (Murphy and Haugen, 1985). Numerous recent studies have shown the importance of the picoplanktonic component, in terms of both

biomass and primary production, in this region as well as in many others (Li *et al.*, 1983; Platt *et al.*, 1983; Glover *et al.*, 1986).

Another cell maximum was observed in the contour plots for the second June transect. At the fourth depth at station 27 (southwest end of the transect) coccolithophorids were relatively abundant (14,000 cells l^{-1}, Fig. 6B), and monads were extremely abundant (180,000 cells l^{-1}, Fig. 7B) in the colder water. However, none of the parameters measured in the Nelson *et al.* (1985) paper showed increases in that sample (see their Fig. 5, station 16), although the subsamples used for counts and the subsamples analyzed by Nelson *et al.* were drawn from the same sample. The Coulter counter was capable of detecting only particles >5 μm and silica containing cells were not abundant there, so those two analytical methods would not be expected to detect this particular cell maximum. The ATP and chlorophyll analyses also failed to detect it, though. Perhaps the population was somewhat senescent, with lower pigment and ATP concentrations than healthy populations. The oxygen contour plot (Fig. 9B) did show elevated oxygen values in the region of this cell maximum, however, so the cells were still photosynthesizing. Large numbers of monads were also present toward the ring edges along the first transect (Fig. 3B).

In general, there was a stong relationship between the physical and biological structure in the ring in June. Maximum phytoplankton abundances were situated above or embedded in the thermocline at ring center, and radial symmetry was apparent. The influence of colder, fresher water was also evident in the intrusions at the ring edge, with coccolithophorids and other algae frequently showing increases in abundance there.

The only stations that clustered distinctly in June were the Slope and Sargasso Sea stations. The ring samples intermingled, and separated more by depth than by location. Deep samples (below the thermocline) separated from shallow samples, and shallow ring center samples separated from shallow ring edge samples. In August, there was some separation based on collection depth, as in June.

Ortner *et al.* (1979) identified and enumerated phytoplankton species from Slope Water, Sargasso Sea, and cold core ring samples. They averaged the cell abundances over all depths and cruises and found the greatest concentrations of cells in the Slope Water, with both the Sargasso Sea and ring values much lower. Correspondence analysis was also performed, and the results varied with season. In the spring and summer, the phytoplankton species composition of the Sargasso Sea and Slope Water sample sets were more similar to each other than either was to the ring set. Although the physical and chemical properties (and euphausid populations) of the ring appeared intermediate between Slope Water and Northern Sargasso Sea conditions, the phytoplankton species composition in the ring was unique and "on no occasion appeared intermediate" in composition. They suggested that this difference was due to the low number of diatoms in the ring relative to the other two regions and postulated that the lack of success of the ring diatoms may have been due to enhanced downward

mixing in the ring. In the fall, the ring and Sargasso Sea samples were more similar to each other than to the Slope Water. These contrasting seasonal patterns may be related to enhanced lateral transport into the ring in the fall due to increased storm activity; such mixing would yield ring and Sargasso Sea samples of more similar composition and reduce the surface signal to satellites. Similar patterns were observed in this study of a warm core ring, with different species and abundances present at the various stations in April, but similar assemblages and abundances at all locations in August.

b. Edge vs. center biomass enhancement. Yentsch and Phinney (1985) postulated that two mechanisms might regulate phytoplankton growth in warm core rings. They believe that the rotary motion of the ring and the sloping isopycnals in the vicinity of the ring edge lead to enhanced nutrient transport into the surface layers. This constant resupply of nutrients leads to near steady state phytoplankton growth at the edge. At ring center, a second mechanism, mixed layer depth, may be the major growth controlling factor. The phytoplankton at center respond to pulsed nutrient input that occurs when the depth of the mixed layer changes, due to either seasonal progression or storm enhanced mixing. The different mechanisms operating at the ring edge and center might enable different phytoplankton groups to dominate in the two regions.

Several earlier ring studies had noted the presence of gelatinous colonies of diatoms of the genus *Thalassiosira* (Fryxell and Gould, 1983; Fryxell *et al.*, 1984, 1985; Gould *et al.*, 1984). These colonies were known from coastal and upwelling areas (Schrader, 1972; Hasle, 1972) and we could not understand why they were present in the supposedly nutrient-poor core water of the ring. We hypothesized that storm-induced upwelling and turbulence were occurring at ring center and were responsible for, or at least played a role in colony formation. These colonies increased in abundance deeper in the water column and toward the center of WCR 82E (Watkins, unpublished observations) and were observed in turbulent, nutrient-rich antarctic waters (Fryxell and Kendrick, 1988). *Leptocylindrus danicus,* a dominant diatom at ring center in June, has also been observed in apparent upwelling regions and responds rapidly to favorable growth conditions (Marshall, 1985; Marshall and Cohn, 1987b).

Now, additional studies have also suggested that nutrients are upwelled at ring center, due to storm activity, an enhanced nitrate gradient at the base of the mixed layer, and a flux from the relaxation of the pycnocline as the ring decays (McCarthy and Nevins, 1986; Franks *et al.*, 1986; Nelson *et al.*, 1988 submitted). In this case, the biology gave an early indication of physical processes occurring in the water column.

Several investigations have also detected enhanced chlorophyll signals at the ring margin (Hoge and Swift, 1983; Tranter *et al.*, 1983; Olson, 1986). The enhanced pigment at the edge of WCR 82B was most pronounced in the spring when the ring was only two months old; the contrast between the edge and the center decreased as the ring aged (Smith and Baker, 1985). In June, the center even exceeded the edge in

chlorophyll biomass. Thus, the spatial and temporal location of biomass maxima may be due to a preference of particular phytoplankton groups for particular regions of the ring, coupled with a seasonal or "ring age" factor. For example, small monads (*Synechococcus, Chlorella*) and coccolithophorids were observed in higher concentrations at the ring periphery in this study, while diatoms were more abundant at the center. The diatom maximum at the center has been observed in five rings now, Gulf Stream rings 82B (this article), 81D, (Fryxell *et al.*, 1985; Gould *et al.*, 1986), and 82E (Watkins, unpublished observations), and East Australian Eddies F and Mario (Jeffrey and Hallegraeff, 1980, 1987). The diatoms may be responding to the upwelling of nutrients at ring center, as mentioned above, and the smaller cells may be responding to an "anticyclogenesis" of nutrients at the ring edge. Anticyclogenesis is associated with the rotary motion of the ring and results in a pumping of nutrients from depth to the surface, along the sloping isopycnals, with energy derived from geostrophic forces (Yentsch and Phinney, 1985). However, the small monads are widely distributed, with highest concentrations generally observed near shore and in Slope Water (Marshall, 1984; Murphy and Haugen, 1985), and the elevated numbers observed at the margin may alternatively be due to advection from the ring exterior.

5. Conclusions

(1) In April, when the water column was well-mixed to 350 m, samples clustered by station, indicating unique species and abundances at each station that were consistent with depth.

(2) A symmetric diatom abundance maximum was observed in the surface waters at ring center in June; dinoflagellate and coccolithophorid cell maxima were located in the thermocline, slightly below the diatom maximum. Phytoplankton distributions mirrored the physical structure of the ring.

(3) The biomass maximum in the Shelf Water entrainment feature that was sampled in June was compositionally distinct from the ring center biomass maximum; different phytoplankton groups dominated in the two regions.

(4) August samples from the ring, Sargasso Sea, Gulf Stream, and Slope Water all contained similar taxa and abundances, although there was some segregation of samples based on collection depth.

(5) Different phytoplankton groups may be responding to different nutrient input mechanisms at the ring edge and center. Diatom maxima at ring center may form as a result of pulsed nutrient input from storms and a slight upwelling due to the gradual relaxation of the thermocline as the ring ages, while concentrations of ultraplanktonic algae (monads, coccolithophorids) toward the ring margin may result from near steady-state nutrient input along sloping isopycnals and/or advection from the ring exterior.

Acknowledgments. We acknowledge Maureen Reap, Sung-Ho Kang and Tiffany Ashworth for their assistance with typing and preparation of figures. Elizabeth Venrick, Rocio Balmori

and Ed Theriot provided stimulating exchange of ideas. Terrence Joyce and Pat Glibert shared their CTD data and phytoplankton samples, respectively. We enjoyed participating in the Warm Core Rings Program and valued the cooperation and interaction with the many investigators involved. Funding was provided by NSF (OCE-81-01785 and OCE 85-03934 to GAF), Sea Grant (University Marine Fellowship to RWG), and the National Research Council (Postdoctoral Associateship to RWG). This work represents part of the dissertation submitted by RWG to Texas A&M University in partial fulfillment of the requirements for the Ph.D. degree.

APPENDIX

Table A-1: Most frequently observed taxa (100) used in principal component analyses.

Bacillariophyceae

Bacteriastrum spp.
Chaetoceros breve Schutt
Chaetoceros spp.
Chaetoceros vixvisibilis Schiller
diatom resting spore
Haslea wawrikae (Hustedt) Simonsen
Leptocylindrus danicus Cleve
Minidiscus trioculatus (F.J.R. Taylor) Hasle
Nitzschia bicapitata Cleve
Nitzschia closterium (Ehrenberg) Smith
Nitzschia pseudodelicatissima Hasle
Nitzschia sicula (Castracane) Hustedt
Nitzschia spp.
Nitzschia subfraudulenta Hasle
Rhizosolenia alata Brightwell
Rhizosolenia delicatula Cleve
Rhizosolenia spp.
Thalassionema nitzschioides Grunow
Thalassiosira bulbosa Syvertsen
Thalassiothrix mediterranea Pavillard
undetermined centric diatom
undetermined diatom
undetermined pennate

Dinophyceae

Ceratium fusus (Ehrenberg) Dujardin
Ceratium tripos O.F. Muller
Cochlodinium spp.
Dinophysis caudata Saville-Kent
Dinophysis tripos Gourret
Flagellate sp. "A"
Glenodinium danicum Paulsen
Gonyaulax braarudii Hasle
Gonyaulax sp. "A"
Gymnodiniaceae
Gyrodinium spp.

Mesoporus perforatus (Gran) Lillick
Mesoporus cf. *perforatus*
Oxytoxum globosum Schiller
Oxytoxum gracile Schiller
Oxytoxum laticeps Schiller
Oxytoxum mediterraneum Schiller
Oxytoxum scolopax Stein
Oxytoxum variabile Schiller
Prorocentrum compressum (Bailey) Abe ex Dodge
Prorocentrum spp.
Prorocentrum sp.?
Prorocentrum triestinum Schiller sensu Taylor
Protoperidinium bipes (Paulsen) Balech
Protoperidinium crassipes (Kofoid) Balech
Protoperidinium deflandrei Lefevre
Protoperidinium tuba (Schiller) Balech
Scrippsiella trochoidea (Stein) Loeblich
Thoracosphaera heimii (Lohmann) Kamptner
Triadinium sphaericum (Murray & Whitting) Dodge
undetermined dinoflagellate

Prymnesiophyceae

Alisphaera ordinata (Kamptner) Heimdal
Anoplosolenia brasiliensis (Lohmann) Deflandre
Anthosphaera oryza (Schlauder) Gaarder
Anthosphaera robusta (Lohmann) Kamptner
Calcidiscus leptoporus (Murray & Blackman) Loeblich
Calciopappas caudatus Gaarder & Ramsfjell
Calciosolenia murrayi Gran
Calyptrolithophora gracillima (Kamptner) Heimdal
Calyptrosphaera catillifera (Kamptner) Gaarder
Caneosphaera molischii (Schiller) Gaarder
Coccolithus pelagicus (Wallich) Schiller
Coronosphaera mediterranea (Lohmann) Gaarder
Discosphaera tubifera (Murray & Blackman) Ostenfeld
Deutschlandia anthos Lohmann
Emiliania huxleyi (Lohmann) Hay
Florisphaera profunda Okada & Honjo
Gephyrocapsa ericsonii McIntyre & Be
Gephyrocapsa oceanica Kamptner
Halopappas adriaticus Schiller
Helladosphaera cornifera (Schiller) Kamptner
Helicosphaera carteri (Wallich) Kamptner
Helicosphaera hyalina Gaarder
Laminolithus marsilii (Borsetti & Cati) Heimdal
Ophiaster hydroideus (Lohmann) Lohmann
Pappsphaera lepida Tangen
Periphyllophora mirabilis (Schiller) Deflandre
Rhabdosphaera clavigera Murray and Blackman

Syracosphaera histrica Kamptner
Syracosphaera pirus Halldal & Markali
Syracosphaera pulchra Lohmann
Thorosphaera flabellata Halldal & Markali
Umbellosphaera irregularis Paasche
Umbellosphaera tenuis (Kamptner) Paasche
undetermined coccolithophorid

Other Algae

cysts
Dictyocha fibula Ehrenberg
eucaryotic cell
monads
Oscillatoria filament
Phaeocystis spp.
Pterosperma spp.
undetermined chrysophytes
undetermined cryptophytes
undetermined flagellates
undetermined prasinophytes
yellow cell

REFERENCES

Barrett, J. R. 1971. Available potential energy of Gulf Stream rings. Deep-Sea Res., *18*, 1221–1231.

Bradford, J. M., R. A. Heath, F. H. Chang and C. H. Hay. 1982. The effect of warm-core eddies on oceanic productivity off northeastern New Zealand. Deep-Sea Res., *29*(12A), 1501–1516.

Bruce, J. G. 1979. Eddies off the Somali coast during the southwest monsoon. J. Geophys. Res., *84*(C12), 7742–7748.

Cresswell, G. R. and R. Legeckis. 1986. Eddies off southeastern Australia. Deep-Sea Res., *33*, 1527–1562.

Evans, R. H., K. S. Baker, O. B. Brown and R. C. Smith. 1985. Chronology of warm-core ring 82B. J. Geophys. Res., *90*(C5), 8803–8811.

Forbes, A. M. G. 1982. A comparison of Kuroshio and East Australian rings. Warm Core Rings Workshop, Wellington, New Zealand.

Franks, P., J. Wroblewski and G. Flierl. 1986. Prediction of enhanced phytoplankton growth due to the frictional decay of a warm core ring. J. Geophys. Res., *91*, 7603–7610.

Fryxell, G. A. and R. W. Gould, Jr. 1983. Field observations on gelatinous colonies of diatoms from six cruises to Gulf Stream warm core rings. J. Phycol., *19s*, 8.

Fryxell, G. A., R. W. Gould, Jr., E. R. Balmori and E. C. Theriot. 1985. Gulf Stream warm core rings: Phytoplankton in two fall rings of different ages. J. Plank. Res., *7*, 339–364.

Fryxell, G. A., R. W. Gould, Jr. and T. P. Watkins. 1984. Gelatinous colonies of the diatom *Thalassiosira* in Gulf Stream warm core rings including *T. fragilis*, sp. nov. Br. Phycol. J., *19*, 141–156.

Fryxell, G. A. and G. A. Kendrick. 1988. Austral spring microalgae across the Weddell Sea ice edge: Spatial relationships found along a northward transect during AMERIEZ 83. Deep-Sea Res., *35*, 1–20.

Fuglister, F. C. 1963. Gulf Stream '60. Prog. Oceanogr., *1*, 265–383.

—— 1972. Cyclonic rings formed by the Gulf Stream, 1965–1966, *in* Studies in Phys. Oceanogr.: A Tribute to George Wust on his 80th Birthday, A. Gordon, ed., Gordon and Breach Science Publishers, New York, 137–138.

—— 1977. A cyclonic ring formed by the Gulf Stream, 1967, *in* A Voyage of Discovery, the George Deacon 70th Anniversary Volume, Supp. to Deep-Sea Res., M. Angel, ed., Pergamon Press, Oxford, 177–198.

Fuglister, F. C. and L. V. Worthington. 1947. Hydrography of the western Atlantic; Meanders and velocities of the Gulf Stream. Woods Hole Oceanogr. Inst. Tech. Rept., WHOI 47-9.

—— 1951. Some results of a multiple ship survey of the Gulf Stream. Tellus, *3,* 1–14.

Glover, H. E., L. Campbell and B. B. Prezelin. 1986. Contribution of *Synechococcus* spp. to size-fractioned primary productivity in three water masses in the Northwest Atlantic Ocean. Mar. Biol., *91,* 193–203.

Gould, R. W., Jr. 1988. Net phytoplankton in a Gulf Stream warm core ring: species composition, relative abundance, and the chlorophyll maximum layer. Deep-Sea Res., (submitted).

Gould, R. W., Jr., E. R. Balmori and G. A. Fryxell. 1986. Multivariate statistics applied to phytoplankton data from two Gulf Stream warm core rings. Limnol. Oceanogr., *31,* 951–968.

Gould, R. W., Jr. and G. A. Fryxell. 1988. Phytoplankton species composition and abundance in a Gulf Stream warm core ring. I. Changes over a five month period. J. Mar. Res., *46,* 367–398, (this issue).

Gould, R. W., Jr., G. A. Fryxell, E. R. Balmori and T. P. Watkins. 1984. A summary of observations on phytoplankton abundance and species composition of warm core rings. EOS, *65,* 912.

Hasle, G. R. 1972. *Thalassiosira subtilis* (Bacillariophyceae) and two allied species. Norw. J. Bot., *19,* 111–137.

Hitchcock, G. L., C. Langdon and T. J. Smayda. 1985. Seasonal variations in the phytoplankton biomass and productivity of a warm-core Gulf Stream ring. Deep-Sea Res., *32,* 1287–1300.

Hoge, F. E. and R. N. Swift. 1983. Airborne dual laser excitation and mapping of phytoplankton photopigments in a Gulf Stream warm core ring. Appl. Opt., *22,* 2272–2281.

Iselin, C. O'D. 1936. A study of the circulation of the western North Atlantic. Pap. Phys. Oceanogr. Met., *4,* 1–101.

Iselin, C. O'D. and F. C. Fuglister. 1948. Some recent developments in the study of the Gulf Stream. J. Mar. Res., *7,* 317–329.

Jeffrey, S. W. and G. M. Hallegraeff. 1980. Studies of phytoplankton species and photosynthetic pigments in a warm core eddy of the East Australian current. I. Summer populations. Mar. Ecol. Prog. Ser., *3,* 285–294.

—— 1987. Phytoplankton pigments, species and light climate in a complex warm-core eddy of the East Australian Current. Deep-Sea Res., *34,* 649–673.

Joyce, T., R. Backus, K. Baker, P. Blackwelder, O. Brown, T. Cowles, R. Evans, G. Fryxell, D. Mountain, D. Olson, R. Schlitz, R. Schmitt, P. Smith, R. Smith and P. Wiebe. 1984. Rapid evolution of a Gulf Stream warm-core ring. Nature, *308,* 837–840.

Joyce, T. M. and S. L. Patterson. 1977. Cyclonic ring formation at the polar front in the Drake Passage. Nature, *265,* 131–133.

Joyce, T. M., R. W. Schmitt and M. C. Stalcup. 1983. Influence of the Gulf Stream upon the short-term evolution of a warm core ring. Aust. J. Mar. Freshw. Res., *34,* 515–524.

Joyce, T. and P. Wiebe. 1983. Warm core rings of the Gulf Stream. Oceanus, *26,* 34-44.

Kirwan, A. D., Jr., W. J. Merrell, Jr., J. K. Lewis and R. E. Whitaker. 1984. Lagrangian

observations of an anticyclonic ring in the western Gulf of Mexico. J. Geophys. Res., *89,* 3417–3424.

Li, W. K. W., D. V. Subba Rao, W. G. Harrison, J. C. Smith, J. J. Cullen, B. Irwin and T. Platt. 1983. Autotrophic picoplankton in the tropical ocean. Science, *219,* 292–295.

Lutjeharms, J. R. E. 1981. Spatial scales and intensities of circulation in the ocean areas adjacent to South Africa. Deep-Sea Res., *28A,* 1289–1302.

McCarthy, J. J. and J. L. Nevins. 1986. Utilization of nitrogen and phosphorus by primary producers in warm-core ring 82-B following deep convective mixing. Deep-Sea Res., *33,* 1773–1788.

Marshall, H. G. 1982. Phytoplankton distribution along the eastern coast of the USA IV. Shelf Waters between Cape Lookout, North Carolina, and Cape Canaveral, Florida. Proc. Biol. Soc. Wash., *95,* 99–113.

—— 1984. Phytoplankton of the northeastern continental shelf of the United States in relation to abundance, composition, cell volume, seasonal, and regional assemblages. Rapp. P.-v. Reun. Cons. Int. Explor. Mer, *183,* 41–50.

—— 1985. Comparison of phytoplankton concentrations and cell volume measurements from the continental shelf off Cape Cod, Massachusetts, U.S.A. Hydrobiologia, *120,* 171–179.

Marshall, H. G. and M. S. Cohn. 1982. Seasonal phytoplankton assemblages in northeastern coastal waters of the United States. NOAA Tech. Memorandum NMFS-F/NEC-15, 31 pp.

—— 1987a. Phytoplankton distribution along the eastern coast of the USA. Part VI. Shelf waters between Cape Henry and Cape May. J. Plank. Res., *9,* 139–149.

—— 1987b. Phytoplankton composition of the New York Bight and adjacent waters. J. Plank. Res., *9,* 267–276.

Mulhearn, P. J. 1983. On the climatology of warm-core rings from the East Australian Current. Aust. J. Mar. Freshw. Res., *34,* 687–692.

Murphy, L. S. and E. M. Haugen. 1985. The distribution and abundance of phototrophic ultraplankton in the North Atlantic. Limnol. Oceanogr., *30,* 47–58.

Nelson, D. M., H. W. Ducklow, G. L. Hitchcock, M. A. Brzezinski, T. J. Cowles, C. Garside, R. W. Gould, Jr., T. M. Joyce, C. Langdon, J. J. McCarthy and C. H. Yentsch. 1985. Distribution and composition of biogenic particulate matter in a Gulf Stream warm-core ring. Deep-Sea Res., *32,* 1347–1369.

Nelson, D. M., J. J. McCarthy, T. M. Joyce and H. W. Ducklow. 1988. Decay of a warm-core ocean eddy increases near surface nutrient availability and primary production. Deep-Sea Res., (submitted).

Newton, J. L., K. Aagaard and L. K. Coachman. 1974. Baroclinic eddies in the Arctic Ocean. Deep-Sea Res., *21,* 707–719.

Nilsson, C. S. and G. R. Cresswell. 1981. The formation and evolution of East Australian Current warm-core eddies. Prog. Oceanog., *9,* 133–183.

Olson, D. B. 1986. Lateral exchange within Gulf Stream warm-core ring surface layers. Deep-Sea Res., *33,* 1691–1704.

Ortner, P. B., E. M. Hulburt and P. H. Wiebe. 1979. Phytohydrography, Gulf Stream rings, and herbivore habitat contrasts. J. Exp. Mar. Biol. Ecol., *39,* 101–124.

Parker, C. E. 1971. Gulf Stream rings in the Sargasso Sea. Deep-Sea Res., *18,* 981–993.

Platt, T., D. V. Subba Rao and B. Irwin. 1983. Photosynthesis of picoplankton in the oligotrophic ocean. Nature, *300,* 702–704.

Ring Group, The (R. H. Backus, G. R. Flierl, D. R. Kester, D. B. Olson, P. L. Richardson, A. C. Vastano, P. H. Wiebe, J. H. Wormuth). 1981. Gulf Stream cold-core rings: Their physics, chemistry, and biology. Science, *212,* 1091–1100.

Schrader, H. J. 1972. *Thalassiosira partheneia,* eine neue Gallertlager bildende zentrale Diatomee, METEOR Forsch.-Ergebn., Reihe D 10, 58–64.

Scott, B. D. 1981. Hydrological structure and phytoplankton distribution in the region of a warm-core eddy in the Tasman Sea. Aust. J. Mar. Freshw. Res., *32,* 479–492.

Simpson, J. J., C. J. Koblinsky, L. R. Haury and T. D. Dickey. 1984. An offshore eddy in the California Current System. Preface. Prog. Oceanog., *13,* 1–4.

Smith, R. C. and K. S. Baker. 1985. Spatial and temporal patterns in pigment biomass in Gulf Stream warm-core ring 82B and its environs. J. Geophys. Res., *90,* 8859–8870.

Tester, L. A. and K. A. Steidinger. 1979. Nearshore marine ecology at Hutchinson Island, Florida: 1971–1974. VII. Phytoplankton, 1971–1973. Florida Marine Research Publication, *34,* 16–61.

Tomosada, A. 1975. Observations of a warm eddy detached from the Kuroshio east of Japan. Bull. Tokai Reg. Fish. Res. Lab., *81,* 13–85.

—— 1978. Oceanographic characteristics of a warm eddy detached from the Kuroshio east of Honsu, Japan. Bull. Tokai Reg. Fish. Res. Lab., *94,* 59–103.

—— 1986. Generation and decay of Kuroshio warm-core rings. Deep-Sea Res., *33,* 1475–1486.

Tranter, D. J., G. S. Leech and D. Airey. 1983. Edge enrichment in an ocean eddy. Aust. J. Mar. Freshw. Res., *34,* 665–680.

Tranter, D. J., G. S. Leech and D. J. Vaudrey. 1982. Biological significance of surface flooding in warm core ocean eddies. Nature, *297,* 572–574.

Tranter, D. J., R. R. Parker and G. R. Cresswell. 1980. Are warm-core eddies unproductive? Nature, *284,* 540–542.

Warm Core Rings Executive Committee, The (G. Flierl, T. Joyce, D. Kester, J. McCarthy, D. Schink, P. Wiebe). 1982. Multidisciplinary program to study warm core rings. EOS, *63,* 834–835.

Yentsch, C. S. and D. A. Phinney. 1985. Rotary motions and convection as a means of regulating primary production in warm core rings. J. Geophys. Res., *90*(C2), 3237–3248.

Yoder, J. A., L. P. Atkinson, T. N. Lee, H. H. Kim and C. R. McClain. 1981. Role of Gulf Stream frontal eddies in forming phytoplankton patches on the outer southeastern shelf. Limnol. Oceanogr., *26,* 1103–1110.

Received: *14 October, 1987;* revised: *3 February, 1988.*